Jia *et al. EURASIP Journal on Wireless Communications and Networking* (2018) 2018:30
https://doi.org/10.1186/s13638-018-1036-2

EURASIP Journal on Wireless Communications and Networking

RESEARCH Open Access

Receiver design combining iteration detection and ICI compensation for SEFDM

Min Jia*†, Zhiying Wu†, Zhisheng Yin, Qing Guo and Xuemai Gu

Abstract

With the rapid development of wireless communication, the spectrum resource becomes rare, and research on utilization of limited spectrum resource becomes more popular, especially in fifth generation (5G) mobile communication system. Some efficient frequency division multiplexing systems, such as spectrally efficient frequency division multiplexing (SEFDM) system, can improve spectrum utilization by further compression of the distance between subcarriers with respect to orthogonal frequency division multiplexing (OFDM) carrier structure. This idea of further compressing bands will efficiently solve the problem of scarce spectrum resource in future. However, this kind of systems exist strong self-caused inter-carrier interference (ICI) due to non-orthogonal subcarriers employment, which poses a great challenge to the design of receiver. In this paper, a receiver designed with iterative ICI compensation (IIC) for SEFDM is proposed, which has excellent bit error rate (BER) performance and low complexity. Simulation results show that the BER performance of system under iterative ICI compensation receiver is almost same as traditional combining iterative detection and fixed sphere detection (ID-FSD) scheme with large bandwidth compression factor (BCF). But the complexity of the proposed method is lower than that of ID-FSD.

Keywords: Non-orthogonal subcarriers, ICI compensation, BER performance, Low complexity

1 Introduction

In multi-carrier transmission systems, orthogonal frequency division multiplexing (OFDM) is always referred to the classical transmission mode with its high spectrum utilization ratio and simple transmission/reception equipment, but fifth generation (5G) requires a transmission system with higher spectrum utilization than OFDM. As an underlying technique, flexible waveforms are required in 5G networks to address the coming challenges. In 5G network, a fundamental requirement of waveform design is to support asynchronous transmission in order to avoid large overhead of synchronization signaling caused by massive terminals. Although OFDM has been used in long-term evolution (LTE), it can hardly meet the above requirements because the orthogonality among subcarriers cannot be maintained in asynchronous transmission.

In 2003, I. Darwazeh proposed a highly efficient frequency division multiplexing technology (SEFDM) [1]. Establishment of this communication system is based on the OFDM system. OFDM system makes the adjacent sub-carriers orthogonal by compressing the sub-carrier spacing appropriately and increases degree of overlap between each other, which saves a lot of spectrum resources. While SEFDM system can improve spectrum utilization by the further compression of the distance between sub-carriers based on OFDM carrier structure [2–4]. The comparison of the spectral structures of the two systems is shown in Fig. 1. If this idea of further compression bands is applied to the next generation of the terrestrial, airborne and satellite communications system, it can solve the problem of rare spectrum resources in future.

SEFDM is one of the candidate technologies for 5G system. However, further compression of the distance between sub-carriers makes the performance of bit error rate (BER) much worse than that of OFDM system with traditional detection method. Efficient spectrum utilization is one of the main research points in 5G. Therefore, it is necessary to further research the related problems in efficiency frequency division multiplexing.

*Correspondence: jiamin@hit.edu.cn
†Equal contributors
Communication Research Center, School of Electronics and Information Engineering, Harbin Institute of Technology (HIT), 150001 Harbin, China

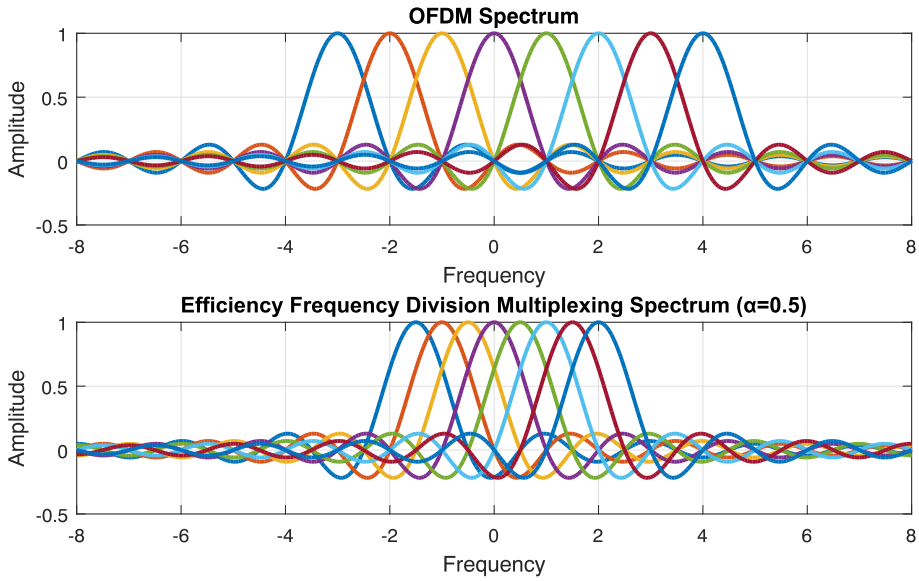

Fig. 1 The comparison of the spectral structures of OFDM and SEFDM with eight subcarriers

Due to the further compression of frequency band, orthogonality between sub-carriers is destroyed, and more complex detection mode is needed to overcome the inter-carrier interference (ICI) and detect the signal [5]. So far, many detection methods for SEFDM system have been proposed such as iterative detection (ID) [6], sphere decoders (SD), truncated singular value decomposition (TSVD), fixed complexity sphere decoder (FSD), combining truncated singular value decomposition and fixed sphere detection (TSVD-FSD) and combining iterative detection and fixed sphere detection (ID-FSD) [7, 8]. All these methods are suitable for SEFDM system [9–12]. However, each detection method has its own disadvantages. For example, the BER performance of ID and SD is worse than that of ID-FSD. But the complexity of ID-FSD is higher than that of ID and FSD. ID-FSD is considered to be the best detection method so far in terms of BER performance.

In this paper, a new receiving method named iterative ICI compensation (IIC) receiver for SEFDM is proposed, which has better BER performance and lower complexity than ID-FSD. The method of iterative ICI compensation receiver is a hybrid one, which combines ID and ICI compensation (IC) receiver.

The rest of this paper is arranged as follows. Section 2 describes the principle of the SEFDM symbol generation and whole frame of traditional SEFDM system. The principle of proposed IC and comparison with other detection methods are depicted in Section 3. Simulation results and conclusion are given in Section 4 and Section 5, respectively.

2 Principle of symbol generation and system model

Figure 2 shows the principle of SEFDM symbol generation [13]. This figure explains how to use inverse Fourier transform to generate SEFDM symbol whose subcarriers are not orthogonal. For example, number of subcarriers is eight, and bandwidth compression factor (BCF). Solid figure in Fig. 2 represents frequency sample points of the 8-point SEFDM symbol. Solid figure and hollow figure represent the frequency sample points of 16-point inverse discrete fourier transform (IDFT) operation. From this figure, we can see that the generation of an 8-carrier frequency-division multiplex symbol is equivalent to an IDFT of 16-point data symbols with 8 invalid data 0 at the end. When the number of subcarriers is same, frequency sample points of each subcarrier in SEFDM symbol are a half of that in OFDM symbol. The diamonds in the figure represent frequency sample points of 8 carrier OFDM symbols.

Figure 3 shows the flow chat of SEFDM system. Considering the generation of a single SEFDM symbol [14], original signal becomes a digital source signal composed of several QAM symbols after sampling, source coding, and constellation mapping. The digital source signal is converted into parallel data by serial-to-parallel conversion. Suppose that parallel data after serial-to-parallel conversion is a N- points data and bandwidth compression factor is α. In order to generate SEFDM symbols, $\frac{1-\alpha}{\alpha}N$ zeros are added to the ends of the N- points data and followed by IDFT of length $\frac{N}{\alpha}$. After IDFT processing, a $\frac{N}{\alpha}$ points data is acquired. Then, at the end $\frac{1-\alpha}{\alpha}N$ points

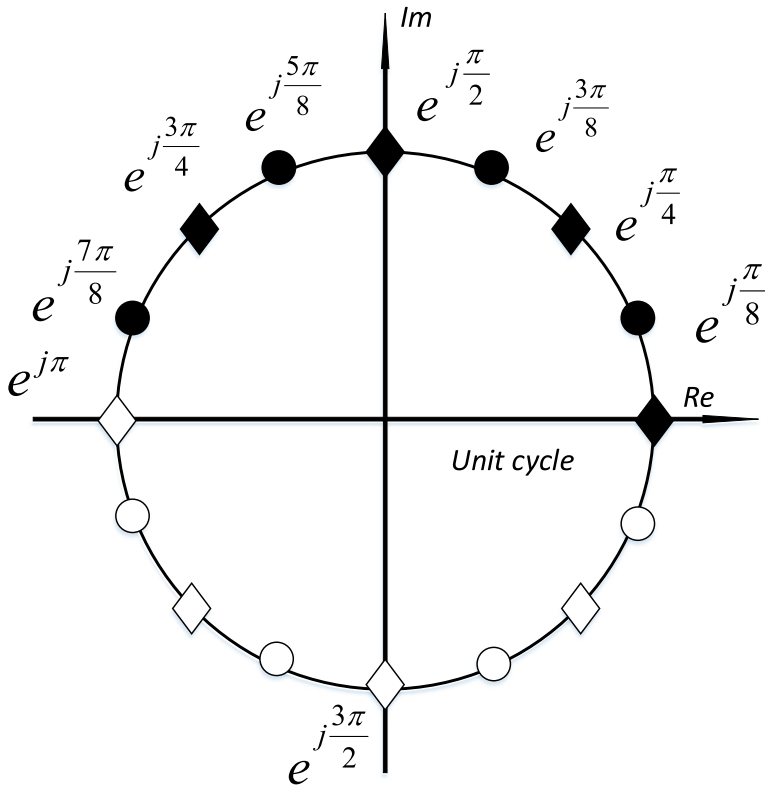

Fig. 2 SEFDM symbol generation schematic

are removed. The remaining N- point data is SEFDM symbol to be transmitted. We regard this algorithm as band compression algorithm.

In the transmitter, complex symbol is generated by symbol mapping and then the SEFDM symbol is generated by band compression algorithm. Specific steps for the process are as follows.

2.1 Symbol mapping

The purpose of symbol mapping is to generate constellation mapping complex symbols, which are mapped into complex symbols by a group of symbols through different modulation schemes by 0, 1. Suppose that number of modulation phase is m, number of transmitted information symbols is n, and the number of complex symbols after mapping is e. After grouping the information 0, 1 binary symbols, each group of symbols is mapped to a complex symbol. Number of binary symbols is h, number of modulation phases of each group is m, and the number of complex symbols after mapping is e, where $h = \log_2 m$, $e = \frac{n}{h}$.

Each group of information symbols are mapped into different constellation points on complex plane by a certain rule, and a group of modulation symbols of different phases is formed. According to the constellation points, increase of the number of original symbol elements of

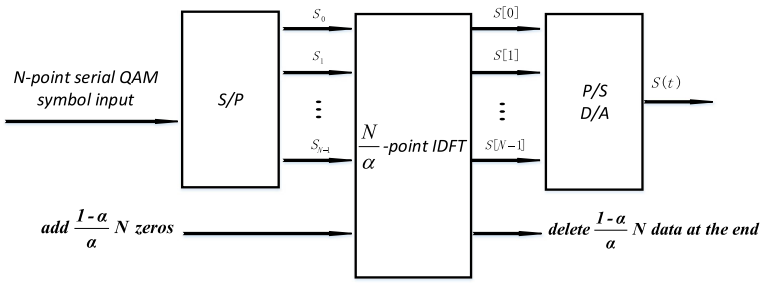

Fig. 3 The generation of SEFDM symbol

each group is equivalent to the improvement upon the transmission efficiency to a certain extent. Under four-phase constellation mapping, mapping rule of the binary inforfig:3mation symbol to the symbol position on thefig:2 complex plane is as follows:

$$Q_{i,k} = (-1)^{i+1}\frac{1}{\sqrt{2}} + j(-1)^{k+1}\frac{1}{\sqrt{2}}, (i = 0, 1; k = 0, 1) \tag{1}$$

Under four-phase constellation mapping, $m = 4$, $h = \log_2 m = 2$. Mapping rule is given as follows:

$$\begin{aligned} &(0,0) \rightarrow e^{j\frac{5\pi}{4}} \\ &(0,1) \rightarrow e^{j\frac{3\pi}{4}} \\ &(1,0) \rightarrow e^{j\frac{7\pi}{4}} \\ &(1,1) \rightarrow e^{j\frac{\pi}{4}} \end{aligned} \tag{2}$$

2.2 Non-orthogonal processing of subcarriers

In this section, the complex symbols are modulated into a set of non-orthogonal subcarriers to generate SEFDM symbols. SEFDM signal is composed of several groups of symbols and each group carrying N complex symbols. T is the cycle of data transmission. Each set of N-dimensional complex symbols is modulated into a set of mutually overlapping, non-orthogonal sub-carriers, and modulated SEFDM signal $x(t)$ has the following form [15]:

$$x(t) = \frac{1}{\sqrt{T}} \sum_{l=-\infty}^{\infty} \sum_{n=0}^{N-1} s_{l,n} e^{j\frac{2\pi n\alpha(t-lT)}{T}} \tag{3}$$

where α is the bandwidth compression factor, $\alpha = \Delta f \times T$; Δf is the subcarrier spacing; T is the SEFDM symbol interval; N is the number of subcarriers; $s_{l,n}$ is the nth subcarrier in the lth SEFDM symbol.

Discrete SEFDM signal $X[k]$ is obtained by sampling the continuous form signal with the sampling interval $\frac{T}{N}$.

$$X_l[k] = \frac{1}{\sqrt{N}} \sum_{n=0}^{N-1} s_{l,n} e^{j\frac{2\pi\alpha nk}{N}} \tag{4}$$

where N is the number of subcarriers and denotes number of sampling points in one period. $X_l[k]$ is the kth time sample point on lth symbol, $1/\sqrt{N}$ is normalization constant. Matrix form of the system is shown as follows:

$$\mathbf{X_l} = \mathbf{\Phi} \times \mathbf{S_l} \tag{5}$$

where $\mathbf{X_l}$ is data vector corresponding to the lth SEFDM symbol, $\mathbf{X_l} = [X_l[0], X_l[1] \ldots\ldots X_l[N-1]]^{\mathrm{T}}$, $\mathbf{S_l}$ is the complex data vector, $\mathbf{S_l} = \left[s_{l,0}, s_{l,1}, s_{l,2}, \ldots, s_{l,N-1}\right]^{\mathrm{T}}$, and $\mathbf{\Phi}$ is a matrix whose size is $N \times N$, which can be represented as follows:

$$\begin{bmatrix} \varphi_{1,1} & \varphi_{1,2} & \cdots & \cdots & \varphi_{1,n} \\ \varphi_{2,1} & \varphi_{2,2} & \cdots & \cdots & \varphi_{2,n} \\ \vdots & \vdots & \ddots & & \vdots \\ \vdots & \vdots & & \ddots & \vdots \\ \varphi_{k,1} & \varphi_{k,2} & \cdots & \cdots & \varphi_{k,n} \end{bmatrix} = \begin{bmatrix} \frac{1}{\sqrt{N}} e^{j\frac{2\pi\alpha 1}{N}} & \frac{1}{\sqrt{N}} e^{j\frac{2\pi\alpha 2}{N}} & \cdots & \cdots & \frac{1}{\sqrt{N}} e^{j\frac{2\pi\alpha n}{N}} \\ \frac{1}{\sqrt{N}} e^{j\frac{2\pi\alpha 2}{N}} & \frac{1}{\sqrt{N}} e^{j\frac{2\pi\alpha 4}{N}} & \cdots & \cdots & \frac{1}{\sqrt{N}} e^{j\frac{2\pi\alpha 2n}{N}} \\ \vdots & \vdots & \ddots & & \vdots \\ \vdots & \vdots & & \ddots & \vdots \\ \frac{1}{\sqrt{N}} e^{j\frac{2\pi\alpha k}{N}} & \frac{1}{\sqrt{N}} e^{j\frac{2\pi\alpha 2k}{N}} & \cdots & \cdots & \frac{1}{\sqrt{N}} e^{j\frac{2\pi\alpha kn}{N}} \end{bmatrix} \tag{6}$$

In other words, the element in the matrix is $\varphi_{k,n} = \frac{1}{\sqrt{N}} e^{j\frac{2\pi\alpha nk}{N}}$, where $0 \le n < N, 0 \le k < N$.

3 Detection methods for SEFDM system

So far, many detection methods for SEFDM system have been proposed such as ID, SD, TSVD, FSD, TSVD-FSD, and ID-FSD [7]. All these methods are suitable for SEFDM system.However, each detection method has its own disadvantages. For example, the BER performance of ID and SD is worse than that of ID-FSD. But the complexity of ID-FSD is higher than that of ID and FSD. ID-FSD is considered to be the best detection method so far in terms of BER performance.

Figure 4 shows the frame of traditional receiver of SEFDM system. This process is opposite to that of transmitter. After the receiver get N- point data with AWGN channel, $\frac{1-\alpha}{\alpha}N$ zeros are added to the end of N- points data and followed by discrete fourier transform (DFT) of length $\frac{N}{\alpha}$. After DFT processing, a $\frac{N}{\alpha}$ points data is acquired. Then, $\frac{1-\alpha}{\alpha}N$ points data are removed at the end. The remaining N-point data is an estimate of the transmitter symbol. Generally, this data should be further processed with, for instance, ID, FSD, TSVD and so on. Further processing is the key to this system in terms of BER performance.

In this paper, an ICI compensation detection is proposed, which has the same BER performance as ID with appropriate number of iterations. In addition, a method that named iterative ICI compensation combining ID and IC is proposed, which has the same BER performance as ID-FSD but has much lower complexity.

The discrete symbol model of SEFDM reception can be represented as:

$$\mathbf{R} = \mathbf{CS} + \mathbf{Z} \tag{7}$$

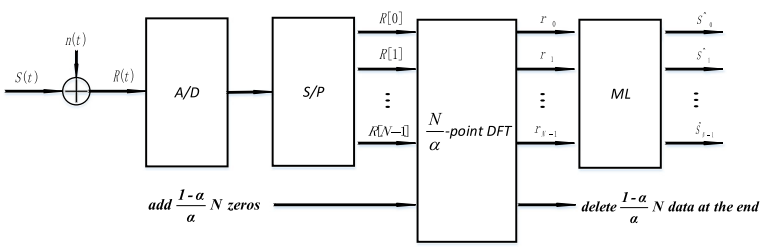

Fig. 4 The traditional receiver of the SEFDM system

where **S** denotes the N-dimensional vector of transmitted symbols, **Z** represents the N-dimensional vector of Gaussian noise, **C** is an $N \times N$ correlation matrix that describes that the interference between the sub-carriers and **R** is an N-dimensional vector of distorted symbols after demodulating the received SEFDM symbols using a DFT operation.

3.1 Iterative detection

ID has a good performance against interference and the mapping strategy is illustrated in Fig. 5 [7]. It can be seen that the whole constellation is divided into Zone A and Zone B. Depending on zones where the received symbols are located in, a different mapping strategy should be employed.

Zone A is more credible to interference compared to Zone B. In Fig. 5 the uncertainty interval is defined by $\Delta d = 1 - m/v$, where m is the m^{th} iteration, v denotes the number of iterations. Only points that fall in Zone A can be mapped to the corresponding constellation point. The points within Zone B keep unchanged and left to the next iteration. The interval is reduced gradually until it reaches zero in the iteration process since the effect of ISI has been canceled out in each iteration. The iterative operation is shown below [7]:

$$\mathbf{S_n} = \mathbf{R} - (\mathbf{C} - \mathbf{e})\mathbf{S_{n-1}} \tag{8}$$

where **R** is the is the symbol matrix received by the receiver; $\mathbf{S_n}$ is an N-dimensional vector of recovered symbols after n iterations, $\mathbf{S_{n-1}}$ is an N-dimensional vector of estimated symbols after $n-1$ iteration, **e** is an $N \times N$ identify matrix.

ID aims to eliminate the ISI step by step. In (8), $\mathbf{S_{n-1}}$ can be seen as an estimate value of **S** and named $\widehat{\mathbf{S}}$

To simplify the problem, assuming that there is no noise, which means $\mathbf{R} = \mathbf{CS}$. Then the equation of ID can be written as:

$$\begin{aligned} \mathbf{S_n} &= \mathbf{R} - (\mathbf{C} - \mathbf{e})\mathbf{S_{n-1}} \\ &= \mathbf{CS} - (\mathbf{C} - \mathbf{e})\widehat{\mathbf{S}} \\ &= \mathbf{CS} - \mathbf{C}\widehat{\mathbf{S}} + \widehat{\mathbf{S}} \\ &= \widehat{\mathbf{S}} - (\mathbf{C}\widehat{\mathbf{S}} - \mathbf{CS}) \end{aligned} \tag{9}$$

Equation (9) shows the principle of the process in ID.

In ID, some symbols in Zone A should be detected after each iteration and replace the initial ones. However, these symbols will be detected again in the next iteration since Zone A becomes larger. It leads to the high complexity in ID. So, a simplified ID algorithm which only uses (8) to get the result may be more accepted in engineering implementation.

From (8) we can get the complexity of ID: the number of complex multiplication operations in per iteration is N^2; the number of complex addition operations in the first iteration is $2N^2$ and the number of complex addition operations in the rest each iteration is N^2. The reason of the phenomenon is that the value of the factor $(\mathbf{C} - \mathbf{e})$ has been calculated in the first iteration, which includes N^2 complex addition operations. Additionally, N is the length of **S**.

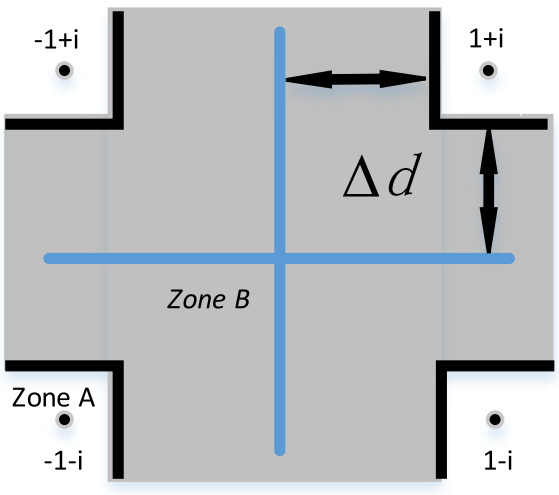

Fig. 5 Mapping strategy

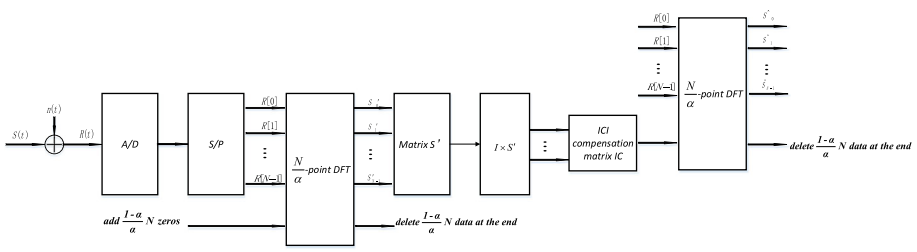

Fig. 6 Receiver for SEFDM with IC

3.2 ICI compensation

The proposed IC is a detection method, which is designed specifically for SEFDM system. Unlike ID, FSD, and some other detection methods, IC aims to optimize the data before the DFT operation. In SEFDM system, some data is deleted after the IDFT operation, which results in non-orthogonal subcarriers. The IC aims to recover the data deleted in the transmitter so as to eliminate the ICI, in other word, compensate the loss caused by ICI. Theoretically, if the deleted data (the deleted $\frac{1-\alpha}{\alpha}N$ data in the transmitter) is recovered completely, the BER performance of SEFDM system will be same as that of OFDM system. The block diagram of receiver with IC is shown in Fig. 6. The block diagram shows IC detection with only one iteration. In practical operation, the number of iterations should be decided based on the actual situation.

As is shown in Fig. 6, a matrix $\mathbf{S}'$, whose initial value is $\mathbf{R}$, is made to be an estimation of matrix $\mathbf{S}$ in the transmitter. We name the ICI compensation matrix $\mathbf{IC}$, which is expressed as :

$$\mathbf{IC} = \mathbf{I} \times \mathbf{S}' \tag{10}$$

where $\mathbf{I}$ is a matrix of size $(K-N) \times N$, which is a block matrix of IDFT matrix. N is the number of subcarriers in one SEFDM symbol, K is the number of points of IDFT, and $K = N/\alpha$. It should be noticed that $\mathbf{I}$ is a bottom left matrix of the IDFT matrix. If each element of the IDFT matrix is expressed as $x_{i,j}$, then the IDFT matrix can be written as:

$$\begin{bmatrix} x_{1,1} & x_{1,2} & \cdots & x_{1,K} \\ x_{2,1} & x_{2,2} & \cdots & x_{2,K} \\ \vdots & \vdots & \ddots & \vdots \\ x_{K-1,1} & x_{K-1,2} & \cdots & x_{K-1,K} \\ x_{K,1} & x_{K,2} & \cdots & x_{K,K} \end{bmatrix} \tag{11}$$

Then matrix $\mathbf{I}$ can be written as:

$$\begin{bmatrix} x_{N+1,1} & x_{N+1,2} & \cdots & x_{N+1,N} \\ x_{N+2,1} & x_{N+2,2} & \cdots & x_{N+2,N} \\ \vdots & \vdots & \ddots & \vdots \\ x_{K-1,1} & x_{K-1,2} & \cdots & x_{K-1,N} \\ x_{K,1} & x_{K,2} & \cdots & x_{K,N} \end{bmatrix} \tag{12}$$

The specific operation process is as follows. In the receiver, $\frac{1-\alpha}{\alpha}N$ zeros are added at the end of $\mathbf{R}$, and followed by the DFT of length $\frac{N}{\alpha}$. After the DFT processing, a $\frac{N}{\alpha}$ points data is acquired. Then, $\frac{1-\alpha}{\alpha}N$ points are removed at the end. The remaining N- point data is an estimate of the matrix $\mathbf{S}$ in transmitter. The matrix $\mathbf{IC}$ is made to add at the end of matrix $\mathbf{R}$ instead of adding zeros and followed by a DFT operation of length $\frac{N}{\alpha}$, which means the first iteration is accomplished. After the processing, the data $\hat{\mathbf{S}}$ is much closer to the real data $\mathbf{S}$. Then, another iteration may be done according to the requirement of the system.

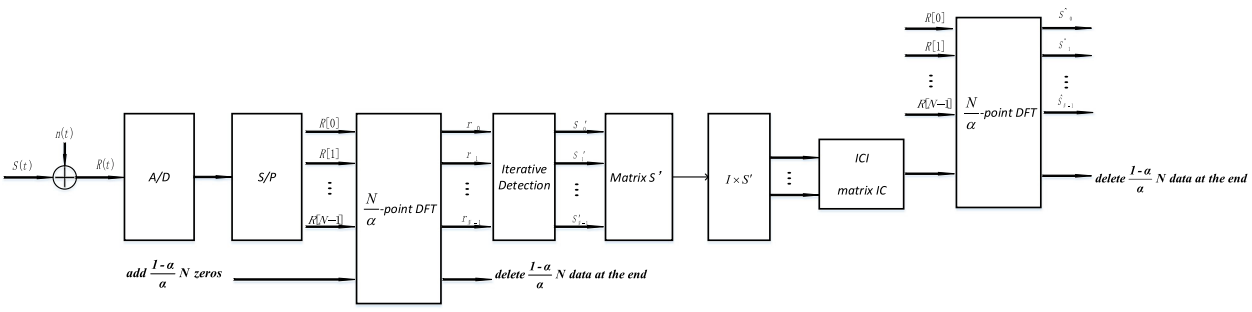

Fig. 7 Receiver for SEFDM with IIC

The complexity of IC is calculated based on its principle. firstly, a block matrix of the $K \times K$ IDFT matrix named $\mathbf{I}$ is acquired. Then, the operation of $\mathbf{I} \times \mathbf{S}'$ is done to get the $\mathbf{IC}$ matrix. After that, the $\mathbf{IC}$ matrix is added at the end of $\mathbf{R}$ instead of adding zeros and followed with a DFT operation. Finally, the result is acquired after removing the $(K - N)$ data at the end.

As the size of matrix $\mathbf{I}$ is small, the amount of computation of $\mathbf{I} \times \mathbf{S}'$ is not large. The number of complex multiplication that $\mathbf{I} \times \mathbf{S}'$ brings in one iteration is $(K - N)N$, and the number of complex addition is $(K-N)(N-1)$. Then, a DFT operation is needed. Generally, the number K is an integer multiple of 2, which can replace DFT with FFT and make the operation more efficient. So, finally, the number of complex multiplication operations in per iteration is $K \log_2^K + (K - N)N$; the number of complex addition operations in one iteration is $K \log_2^K + (K - N)(N - 1)$.

It should be noticed that the matrix $\mathbf{IC}$ is generated by $\mathbf{I} \times \mathbf{S}'$ and $\mathbf{S}'$ is made up of useful data after the DFT operation other than the ignored data.

3.3 ID-FSD detection

Firstly, an initial radius is required which determines the size of the search sphere, as in the equation below [7]:

$$\breve{g}_{ID} = ||\mathbf{R} - \mathbf{C}\bar{\mathbf{S}}||^2 \tag{13}$$

where $||\bullet||$ donates the Euclidean norm. The initial radius equals the distance between the sphere center and the initial constrained estimate $\bar{\mathbf{S}}$. Due to the ill conditioning of SEFDM system, these initial estimates may deviate greatly from the optimal points. Therefore, ID is employed to calculate an improved initial radius.

The FSD block implements the SEFDM detection algorithm using equation:

$$\tilde{\mathbf{S}}_{\mathbf{ID-FSD}} = \arg \min_{\tilde{\mathbf{S}} \in \mathbf{O}^N} ||\mathbf{R} - \mathbf{C}\tilde{\mathbf{S}}||^2 \leq \breve{g}_{ID} \tag{14}$$

where $\tilde{\mathbf{S}}$ is a detected symbol vector, $\mathbf{O}$ is the constellation cardinality and $\breve{g}_{ID}$ is the initial radius transferred from FSD-initializer. If finally no node is found within the sphere, the ID constrained estimate is taken as the solution $\bar{\mathbf{S}}$, as expressed in the equality below:

$$\tilde{\mathbf{S}}_{\mathbf{ID-FSD}} = \bar{\mathbf{S}} \tag{15}$$

This is why the design contains a feed of the constrained estimates from ID-Processor to the FSD block. In order to simplify the squared Euclidean norm calculation, Eq. (14) can be transformed into an equivalent expression using Cholesky decomposition. The transformation is carried out using $chol\{\mathbf{C} * \mathbf{C}\} = \mathbf{L} * \mathbf{L}$, where $\mathbf{L}$ is an $N \times N$ upper triangular matrix. Hence, (14) can be re-written as [7]:

$$\tilde{\mathbf{S}}_{\mathbf{ID-FSD}} = \arg \min_{\tilde{\mathbf{S}} \in \mathbf{O}^N} ||\mathbf{L}(\hat{\mathbf{S}} - \tilde{\mathbf{S}})||^2 \leq \breve{g}_{ID} \tag{16}$$

The elements of $\mathbf{C}$ and Cholesky decomposition of $\mathbf{C}$ are stored in this block, where $c_{m,n}$ are the elements of $\mathbf{C}$ and are used for calculating the initial radius in Eq. (13). $l_{m,n}$ denotes the elements of the upper triangular matrix and are used for calculating squared Euclidean norm in Eq. (16).

Additionally, QR decomposition is an alternative method to transform Eq. (14). The transformation is carried out using $\mathbf{C} = [\mathbf{Q_1}, \mathbf{Q_2}] \begin{bmatrix} \mathbf{R_u} \\ \mathbf{0} \end{bmatrix}$, where $\mathbf{R_u}$ is an $N \times N$ upper triangular matrix, $[\mathbf{Q_1}, \mathbf{Q_2}]$ is an $\frac{N}{\alpha} \times \frac{N}{\alpha}$ unitary matrix and $\mathbf{Q_1}$ is a $\frac{N}{\alpha} \times N$ matrix. Suppose that $\begin{cases} \mathbf{y} = \mathbf{Q_1^H R} \\ \breve{g}_{ID2} = \breve{g}_{ID} - ||\mathbf{Q_2^H R}||^2 \end{cases}$, (14) can be re-written as:

$$\tilde{\mathbf{S}}_{\mathbf{ID-FSD}} = \arg \min_{\tilde{\mathbf{S}} \in \mathbf{O}^N} ||\mathbf{y} - \mathbf{R_u}\tilde{\mathbf{S}}||^2 \leq \breve{g}_{ID2} \tag{17}$$

Actually, it's too complex to consider all of the situations when deciding the value of each dimension in FSD. Therefore, a simplified FSD is implemented in the paper. The simplified method decides an exact value instead of a range from the last dimension to the first dimension. It makes the complexity much lower. However, this method performs well only when the size of the system is small.

3.4 IIC detection

The principle of ICI compensation detection has been described above. Matrix $\mathbf{IC}$ is the key to the performance of the system. Matrix $\mathbf{S}'$ determines the accuracy of $\mathbf{IC}$.

Table 1 Complexity comparison

	ID	FSD	IC
Multiplications	N^2	$N^3 + N^2 + NM$	$K \log_2^K + (K - N)N$
Additions	N^2	$N^3 + N^2 - N + NM - M$	$K \log_2^K + (K - N)(N - 1)$

Table 2 Simulation parameters

Detector	FFT size	Subcarrier number	α
ID	8	7,6	7/8,6/8
FSD	8	7,6	7/8,6/8
IC	8	7,6	7/8,6/8
ID-FSD	8	7,6	7/8,6/8
IIC	8	7,6	7/8,6/8

Table 3 Simulation parameters

Detector	FFT size	Subcarrier number	α
ID	16	15,14	15/16,14/16
FSD	16	15,14	15/16,14/16
IC	16	15,14	15/16,14/16
ID-FSD	16	15,14	15/16,14/16
IIC	16	15,14	15/16,14/16

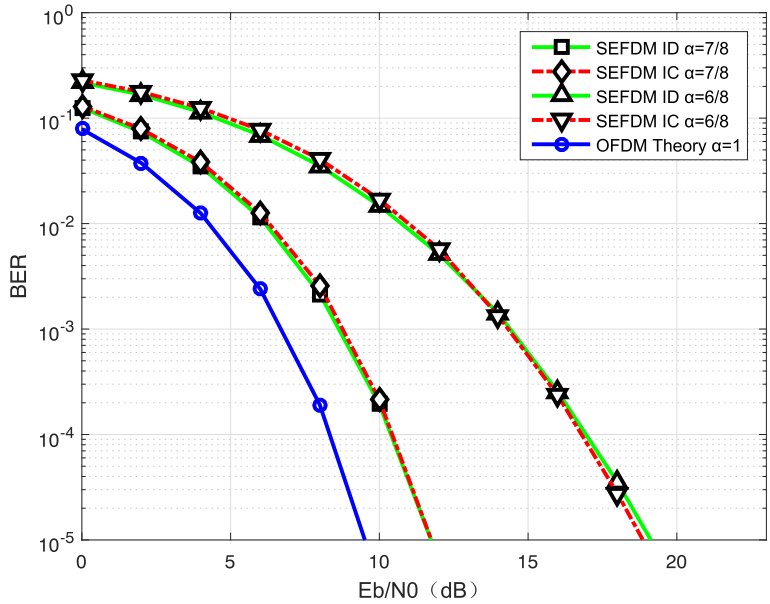

Fig. 8 Comparison of different SEFDM symbol detection schemes

So, if matrix $\mathbf{S}'$ is an excellent estimation of real data, the performance of ICI compensation detection will be much better. For this, an improved method named IIC is proposed in this paper. The flow chart of the receiver with IIC is shown in Fig. 7.

The IIC combines ID and IC detection. Before performing the IC operation, an ID operation is done, which can provide a more accurate initial data for IC detection. When combined with ID, the number of iterations in IC can be reduced drastically, even to only once, which result in the lower complexity.

4 Simulation results

The performance and complexity of ID, FSD, and proposed detector are evaluated. The work in this paper is to test the performance of our system. Therefore, 4-QAM

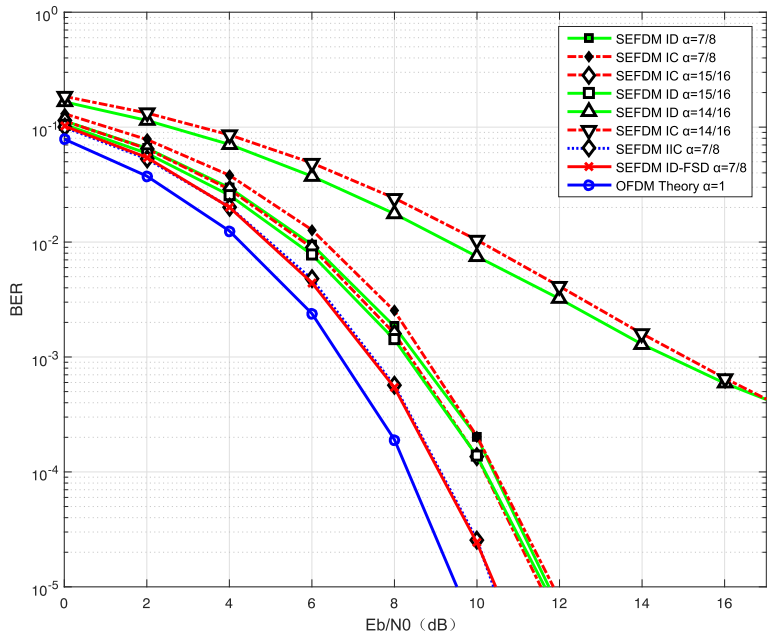

Fig. 9 Comparison of different SEFDM symbol detection schemes

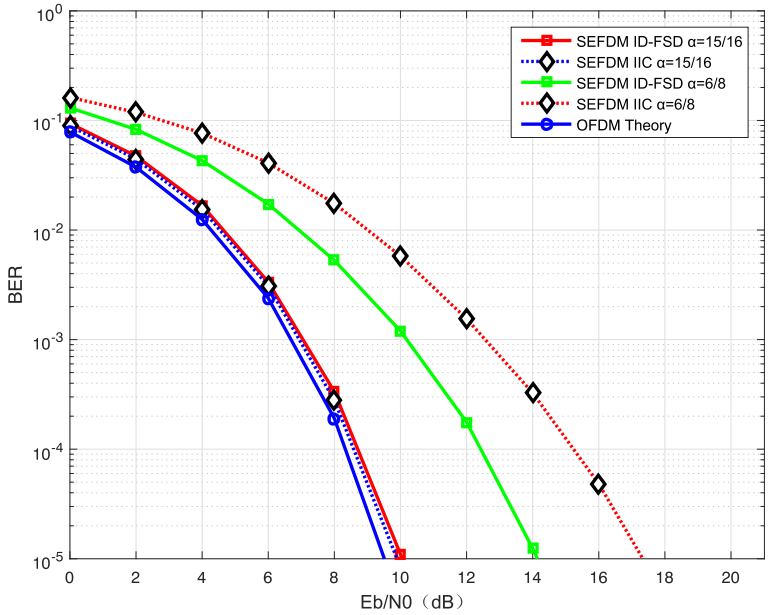

Fig. 10 Comparison of different SEFDM symbol detection schemes

modulation scheme is adopted throughout the simulations and only an AWGN channel is assumed. Table 1 presents the complexity in terms of complex-valued multiplications and complex-valued additions. Some other parameters in the simulation are shown in Tables 2 and 3.

Figure 8 shows the BER performance of IC and ID schemes with $\alpha = 7/8$, 7 useful subcarriers and $\alpha = 6/8$, 6 useful subcarriers, in SEFDM system. Theoretical BER curve of OFDM system is shown in the figure for comparison. In this simulation, the number of iteration is 15 when $\alpha = 7/8$ and 50 when $\alpha = 6/8$ in both ID and IC.

Figure 9 shows the BER performance of IC and ID schemes with $\alpha = 15/16$, 15 useful subcarriers, $\alpha = 14/16$, 14 useful subcarriers, and the BER performance of four different detection schemes with $\alpha = 7/8$, 7 useful subcarriers in SEFDM system. Theoretical BER curve

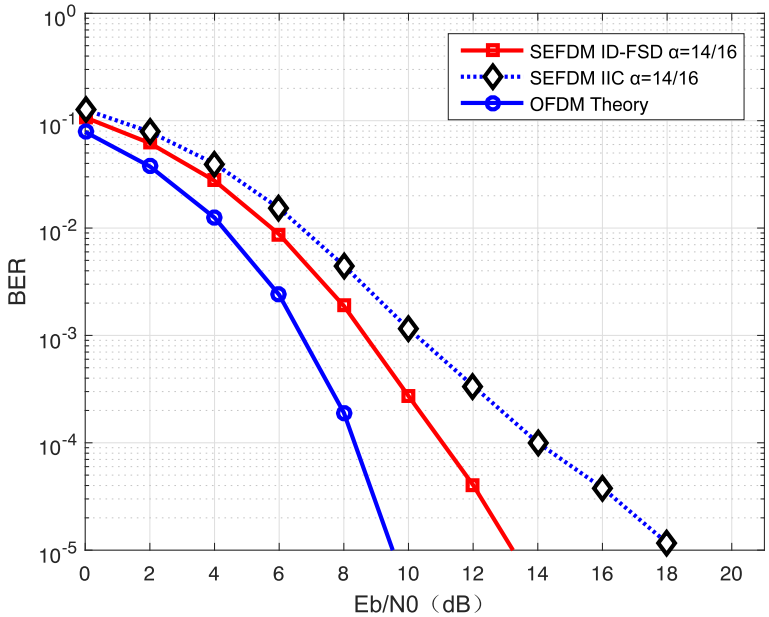

Fig. 11 Comparison of different SEFDM symbol detection schemes

of OFDM system is shown in the figure for comparison. In this simulation, the number of iteration is 15 when $\alpha = 15/16$; 100 when $\alpha = 14/16$ in ID and IC; in IIC the number of iteration is 10 in ID, and 1 in IC. Figures 8 and 9 illustrate that BER performance of ID is almost same as that of IC. However, the computational complexity of IC is much lower than that of ID. Additionally, from Fig. 9 we can see that under the detection of IIC, the system has the same BER performance as that under ID-FSD with $\alpha = 7/8$ and 7 useful subcarriers in SEFDM system. But the complexity of IIC is much lower than that of ID-FSD.

Figures 8 and 9 illustrate that BER performance of ID is almost same as that of IC. However, the computational complexity of IC is much lower than that of ID.

Figure 10 shows the BER performance of ID-FSD and IIC schemes with $\alpha = 6/8$, 6 useful subcarriers and $\alpha = 15/16$, 15 useful subcarriers in SEFDM system. Theoretical BER curve of OFDM system is shown in figure for comparison. In this simulation, the number of iteration is 50 in ID, and 1 in IC when $\alpha = 6/8$ and the number of iteration is 10 in ID, 1 in IC when $\alpha = 15/16$. Figure 10 shows that when $\alpha = 6/8$ and six subcarriers are useful in SEFDM system, the BER performance of ID-FSD is better than that of IIC. Only when the SNR is much larger, the BER can achieve an acceptable value in IIC. Additionally, from Fig. 10, we can see that under the detection of IIC, the system has the same BER performance as that under ID-FSD with $\alpha = 15/16$ and 15 useful subcarriers in SEFDM system. But the complexity of IIC is much lower than that of ID-FSD.

Figure 11 shows the BER performance of different detection schemes with $\alpha = 14/16$ and 14 useful subcarriers in SEFDM system. Theoretical BER curve of OFDM system is shown in the figure for comparison. In the simulation of IIC, the number of iteration is 100 in ID, and 1 in IC and in ID-FSD the number of iteration is 10 in ID. Figure 11 shows that when $\alpha = 14/16$ and 14 subcarriers are useful in SEFDM system, the BER performance of ID-FSD is better than that of IIC. Only when the SNR is much larger, the BER can achieve an acceptable value in IIC.

It can be seen from these figures that in case of small α, more iterations are required to converge the BER curve, and increase the number of subcarriers means the increase of ICI strength, which makes the performance of BER worse.

5 Conclusions

SEFDM yields higher spectral efficiency than OFDM by employing non-orthogonal sub-carriers. The deliberate collapse of orthogonality property in SEFDM systems necessitates more complicated detectors. A new detector named ICI compensation is proposed in this paper, which has better BER performance than iterative detection. Finally, a hybrid detector named iterative ICI compensation is proposed and achieves better BER performance and lower complexity than ID-FSD. However, the IIC method has the similar performance as ID-FSD only when the value of α is large.

Acknowledgements
This work was supported by National Natural Science Foundations of China (No.61671183, 61771163 and 91438205) and the Open Fund of Shanghai Key Laboratory of Integrated Administration Technologies for Information Security (AGK201706).

Authors' contributions
ZYW wrote the majority of the text and performed the design and implementation of the algorithm. QG and XMG contributed text to earlier versions of the manuscript and participated in the theoretical analysis. MJ and ZSY commented on and approved the manuscript. ZYW and ZSY initiated the research on the detection of IC. All authors read and approved the final manuscript.

Competing interests
The authors declare that they have no competing interests.

Publisher's Note

Received: 10 October 2017 Accepted: 20 January 2018
Published online: 05 February 2018

References

1. I Darwazeh, M Rodrigues, in *(Proceedings) 8th International OFDM-Workshop (InOWo'03)*. A Spectrally Efficient Frequency Division Multiplexing Based Communications System (Hamburg, 2003), pp. 70–74
2. I Darwazeh, T Xu, T Gui, Y Bao, Z Li, Optical SEFDM System; Bandwidth Saving Using Non-Orthogonal Sub-Carriers. IEEE Photon. Technol. Lett. **26**(4), 352–355 (2014)
3. T Xu, I Darwazeh, in *2014 9th International Symposium on Communication Systems, Networks & Digital Sign (CSNDSP)*. Multi-band reduced complexity spectrally efficient FDM systems, (Manchester, 2014), pp. 982–987
4. SV Zavjalov, SB Makarov, SV Volvenko, *et al*, in *Internet of Things, Smart Spaces, and Next Generation Networks and Systems*. Efficiency of coherent detection algorithms non-orthogonal multi-frequency signals based on modified decision diagram (Springer International Publishing, 2015)
5. I Kanaras, A Chorti, M Rodrigues, *et al*, *Analysis of Sub-optimum detection techniques for a bandwidth efficient multi-carrier communication system*, vol. 5, (2008), pp. 1310–1316
6. D Dasalukunte, F Rusek, V Owall, in *Proc. of IEEE International Conference on Communications (ICC)*. 2010 IEEE International Conference on Communications, (Cape Town, 2010), pp. 1–5
7. T Xu, RC Grammenos, F Marvasti, I Darwazeh, An Improved Fixed Sphere Decoder Employing Soft Decision for the Detection of Non-orthogonal Signals. IEEE Commun. Lett. **17**(10), 1964–1967 (2013)
8. A Rashich, D Fadeev, in *International Conference on Next Generation Wired/Wireless Networking*. Optimal Input Power Backoff of a Nonlinear Power Amplifier for FFT-Based Trellis Receiver for SEFDM Signals (Springer International Publishing, 2016), pp. 641–647
9. I Kanaras, A Chorti, M Rodrigues, *et al*, Analysis of sub-optimum detection techniques for bandwidth efficient multi-carrier communication system. SAE Int. J. Fuels Lubr. **5**(3), 1310–1316 (2008)
10. RC Grammenos, S Isam, I Darwazeh, in *2011 IEEE 22nd International Symposium on Personal*. FPGA design of a truncated SVD based receiver for the detection of SEFDM signals (Indoor and Mobile Radio Communications, Toronto, 2011), pp. 2085–2090
11. MR Perrett, I Darwazeh, in *2011 18th International Conference on Telecommunications*. Flexible hardware architecture of SEFDM transmitters with real-time non-orthogonal adjustment (Ayia Napa, 2011), pp. 369–374

12. PN Whatmough, MR Perrett, S Isam, I Darwazeh, in *IEEE Transactions on Circuits and Systems I: Regular Papers, vol. 59, no. 5*. VLSI Architecture for a Reconfigurable Spectrally Efficient FDM Baseband Transmitter (Circuits and Syst, 2012), pp. 1107–1118
13. PN Whatmough, MR Perrett, S Isam, I Darwazeh, VLSI Architecture for a Reconfigurable Spectrally Efficient FDM Baseband Transmitter. IEEE Trans. Circ. Syst. I: Regular Papers. **59**(5), 1107–1118 (2012)
14. S Isam, I Kanaras, I Darwazeh, in *2011 IEEE Wireless Communications and Networking Conference*. A Truncated SVD approach for fixed complexity spectrally efficient FDM receivers, (Cancun, Quintana Roo, 2011), pp. 1584–1589
15. T Xu, I Darwazeh, Transmission Experiment of Bandwidth Compressed Carrier Aggregation in a Realistic Fading Channel. EEE Trans. Veh. Technol. **66**(5), 4087–4097 (2017)